Nickel Foam Supported Porous Copper Oxide Catalysts with Noble Metal-like Activity for Aqueous Phase Reactions

Lorianne R. Shultz,[a] Konstantin Preradovic,[a] Suvash Ghimire,[b] Hayden M. Hadley,[a] Shaohua Xie,[c] Varchaswal Kashyap,[b] Melanie J. Beazley,[a] Kaitlyn E. Crawford,[a,b,c,d] Fudong Liu,*[c,e,f] Kausik Mukhopadhyay,*[b] Titel Jurca*[a,c,f]

a. Department of Chemistry, University of Central Florida, Orlando, Florida, 32816 (USA), E-mail: Titel.Jurca@ucf.edu
b. Department of Materials Science and Engineering, University of Central Florida Orlando, Florida, 32816 (USA), E-mail: Kausik@ucf.edu
c. NanoScience and Technology Center (NSTC), University of Central Florida Orlando, Florida, 32826 (USA)
d. Biionix Faculty Cluster, University of Central Florida, Orlando, Florida, 32816 (USA)
e. Department of Civil, Environmental, and Construction Engineering, University of Central Florida, Orlando, Florida, 32816 (USA) E-mail: Fudong.Liu@ucf.edu
f. Renewable Energy and Chemical Transformation Faculty Cluster (REACT), University of Central Florida, Orlando, Florida, 32816 (USA)

Table of Contents

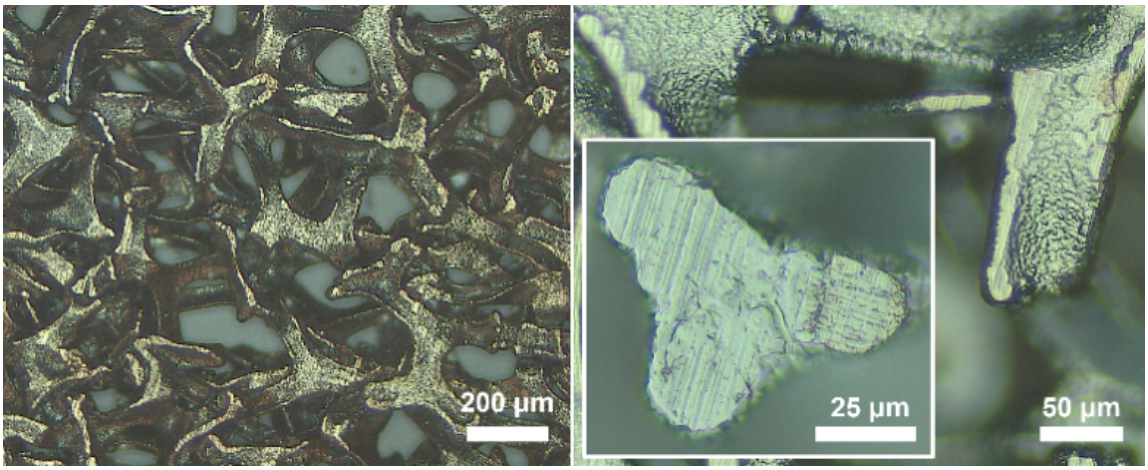

Figure S1. Optical microscope image of untreated nickel foam as purchased from MTI Corporation; < 20% porosity, 80 µm thick.

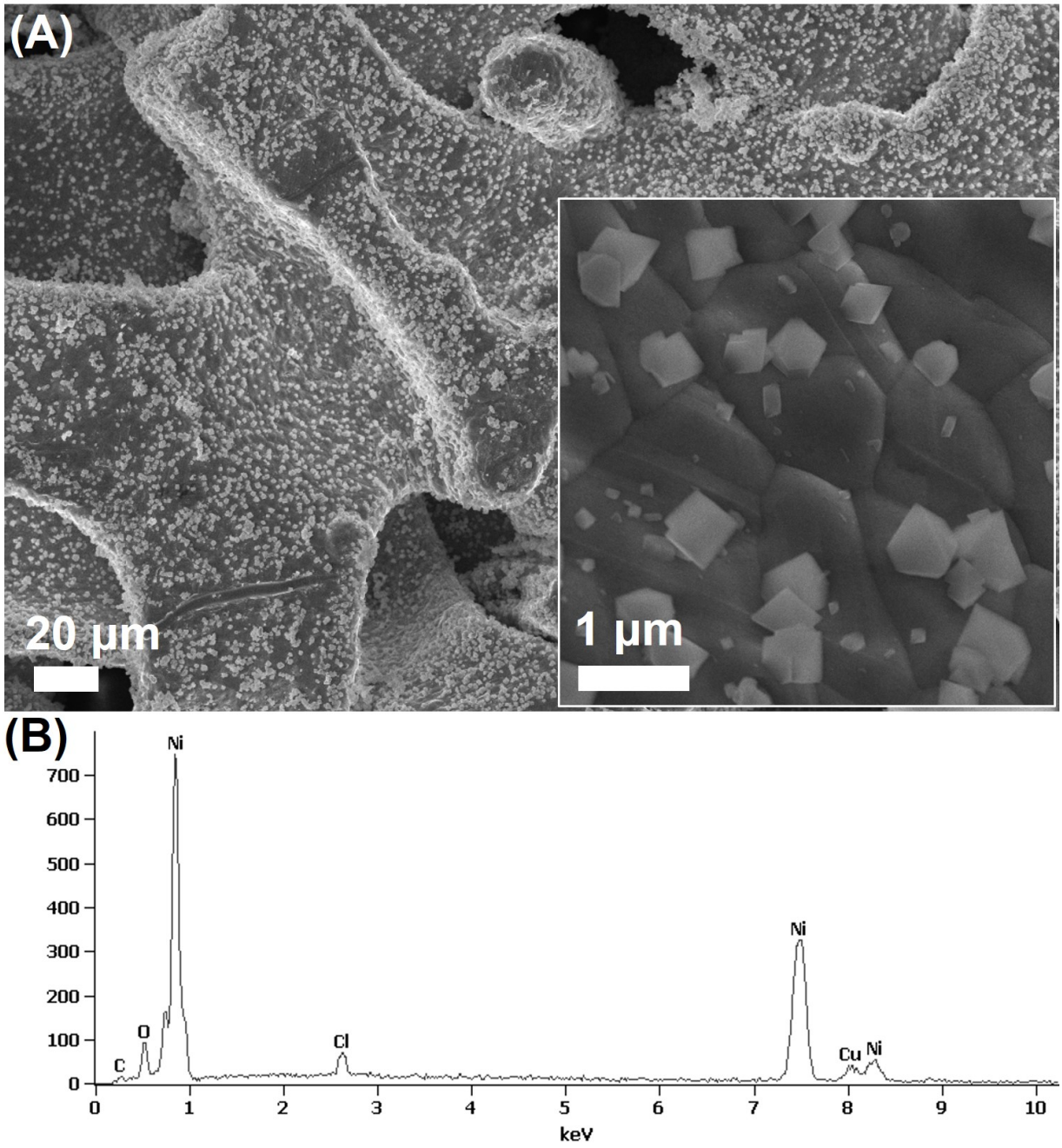

Figure S2: SEM micrograph (A) and EDS spectrum (B) of **Cu/Ni$_{200}$**.

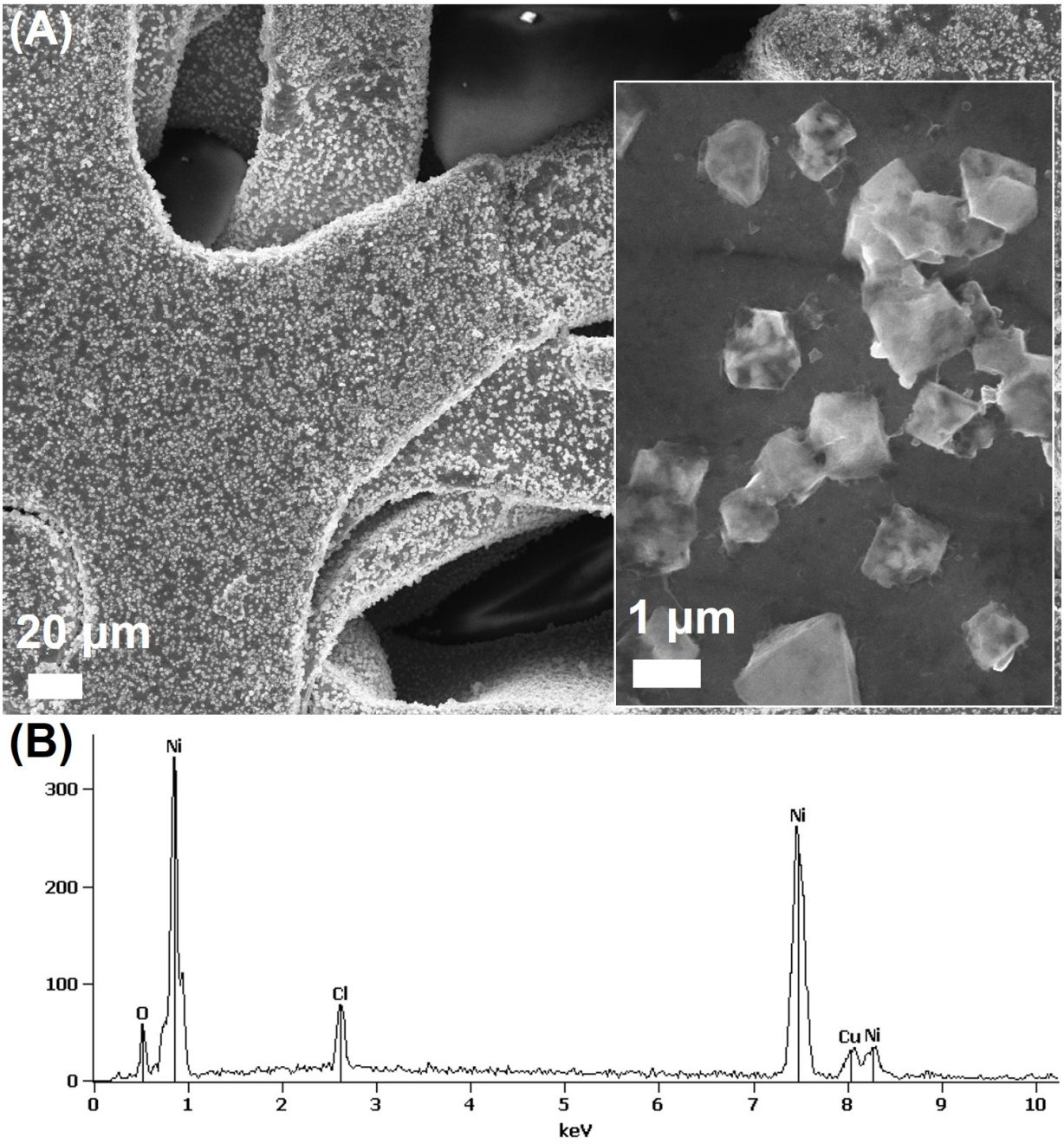

Figure S3: SEM micrograph (A) and EDS spectrum (B) of **Cu/Ni$_{300}$**.

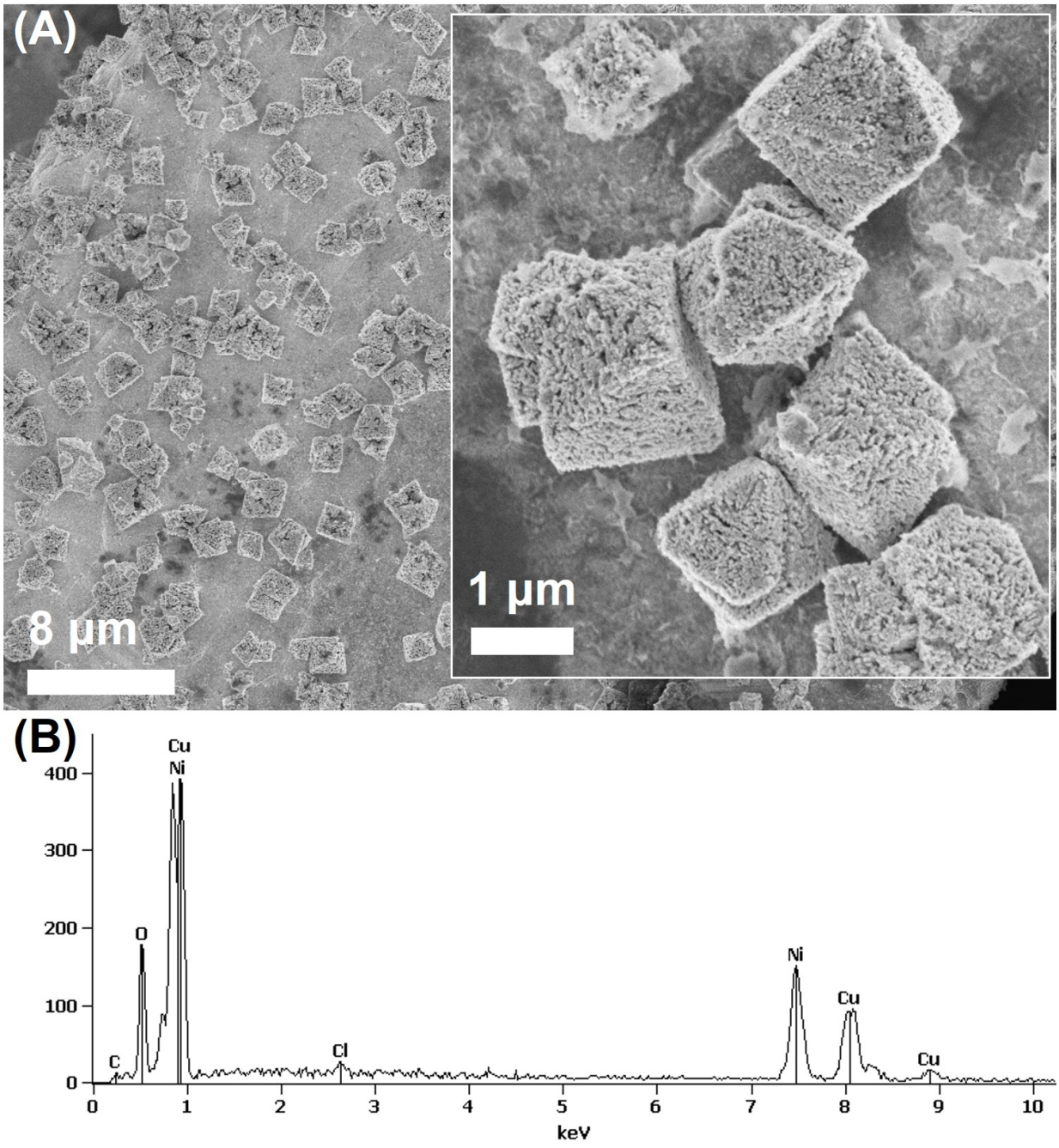

Figure S4: SEM micrograph (A) and EDS spectrum (B) of **Cu/Ni$_{400}$**.

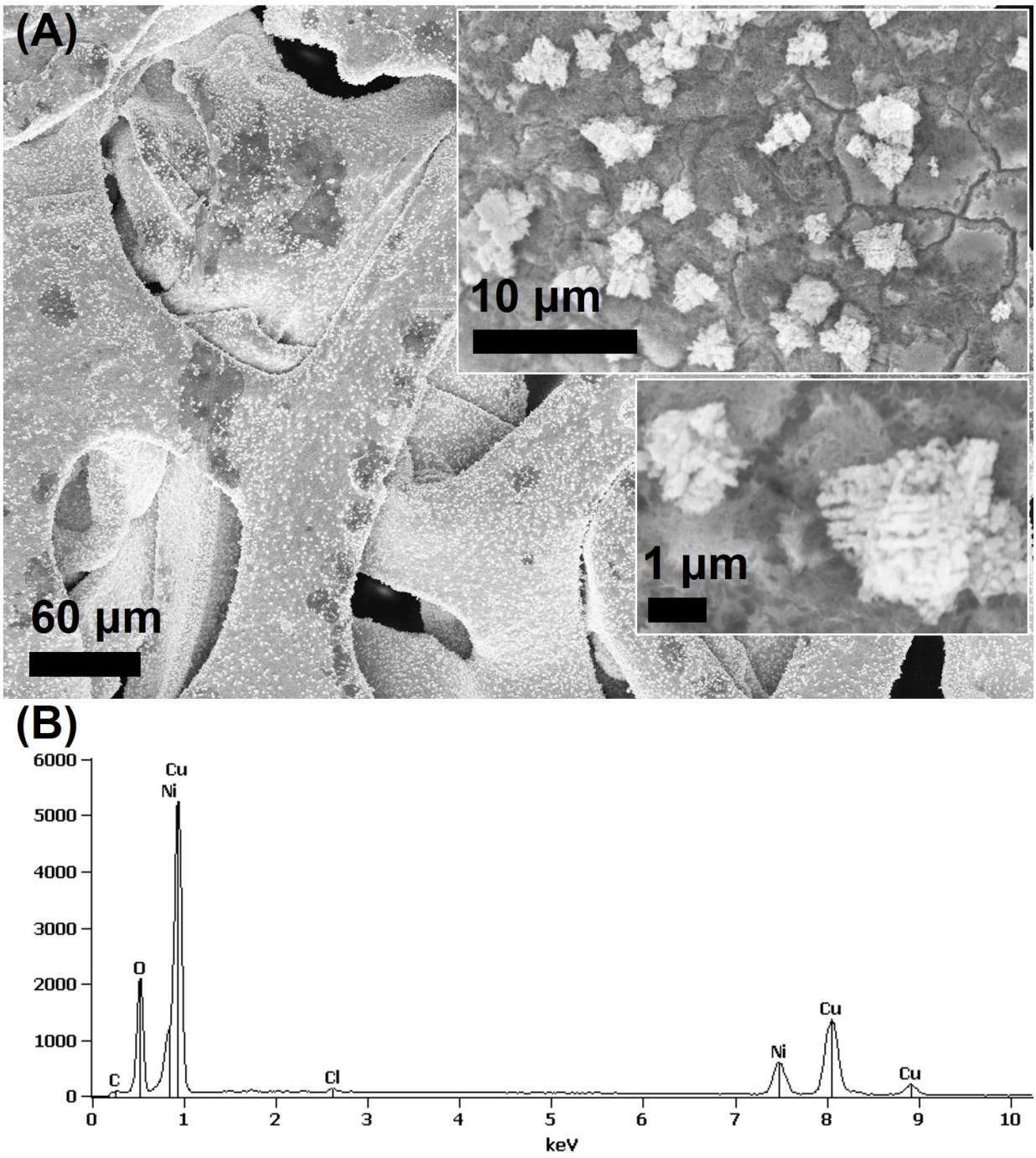

Figure S5: SEM micrograph (A) and EDS spectrum (B) of **Cu/Ni$_{500}$**.

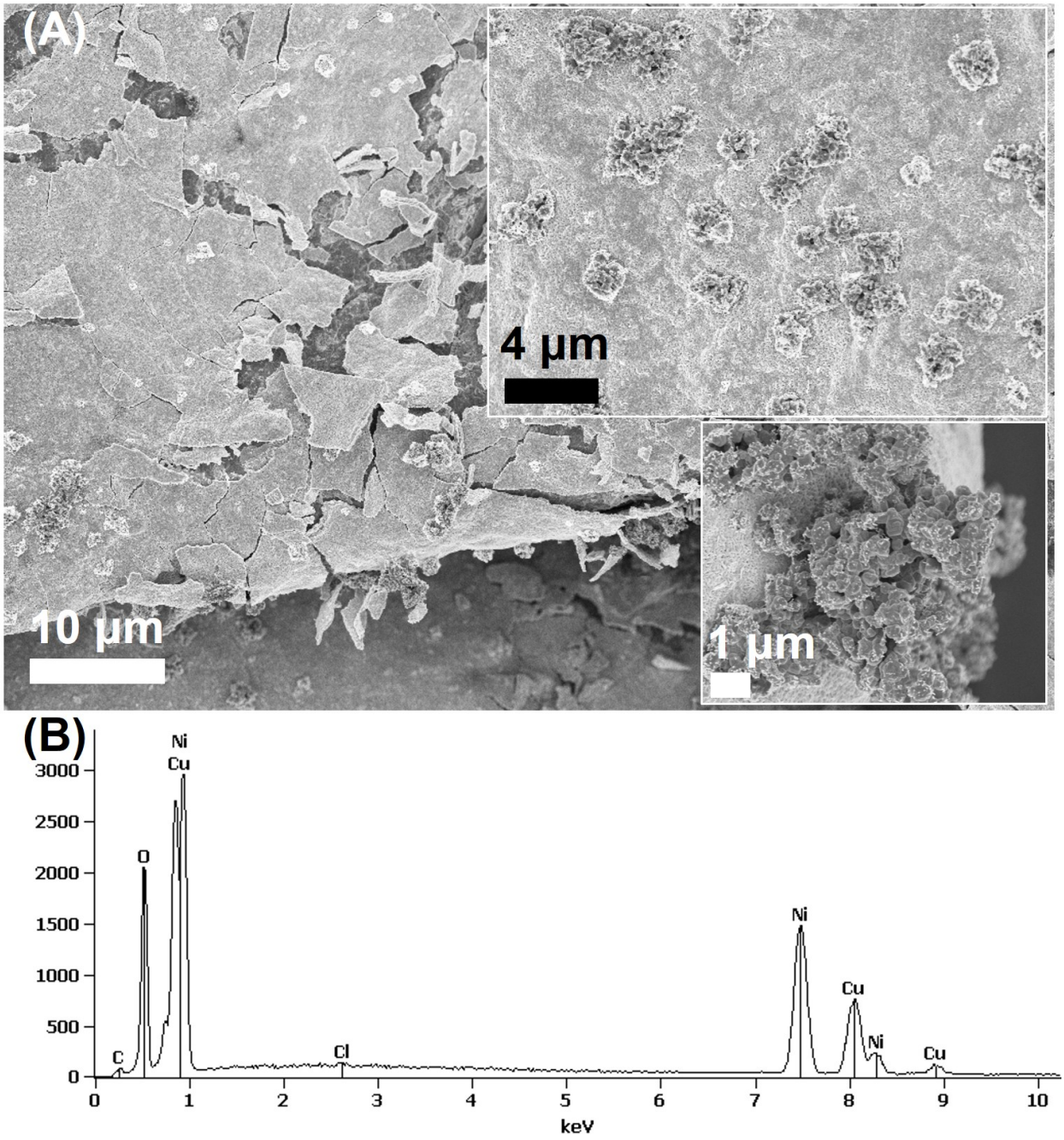

Figure S6: SEM micrograph (A) and EDS spectrum (B) of **Cu/Ni$_{600}$**.

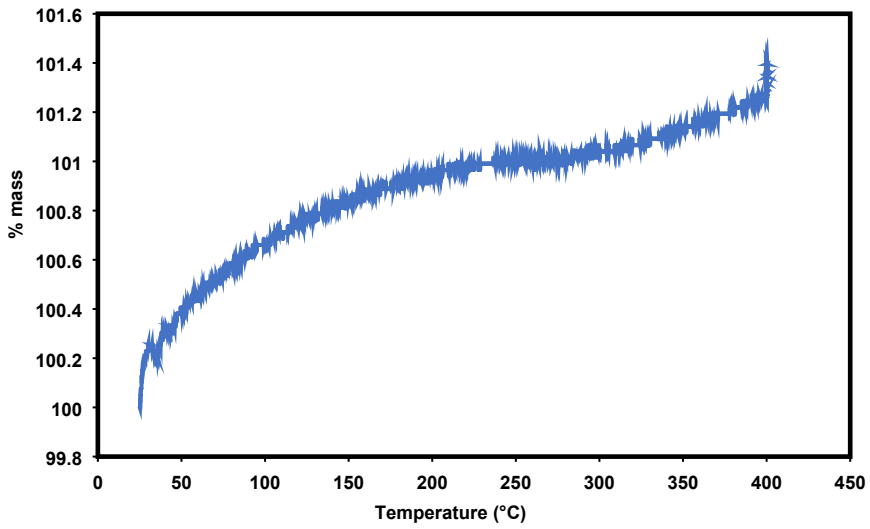

Figure S7: Thermogravimetric curve for bare Ni foam conducted under air with a heating rate of 5 °C/minute with a 60-minute hold at 400 °C. *Increased mass indicates formation of nickel oxide on surface.*

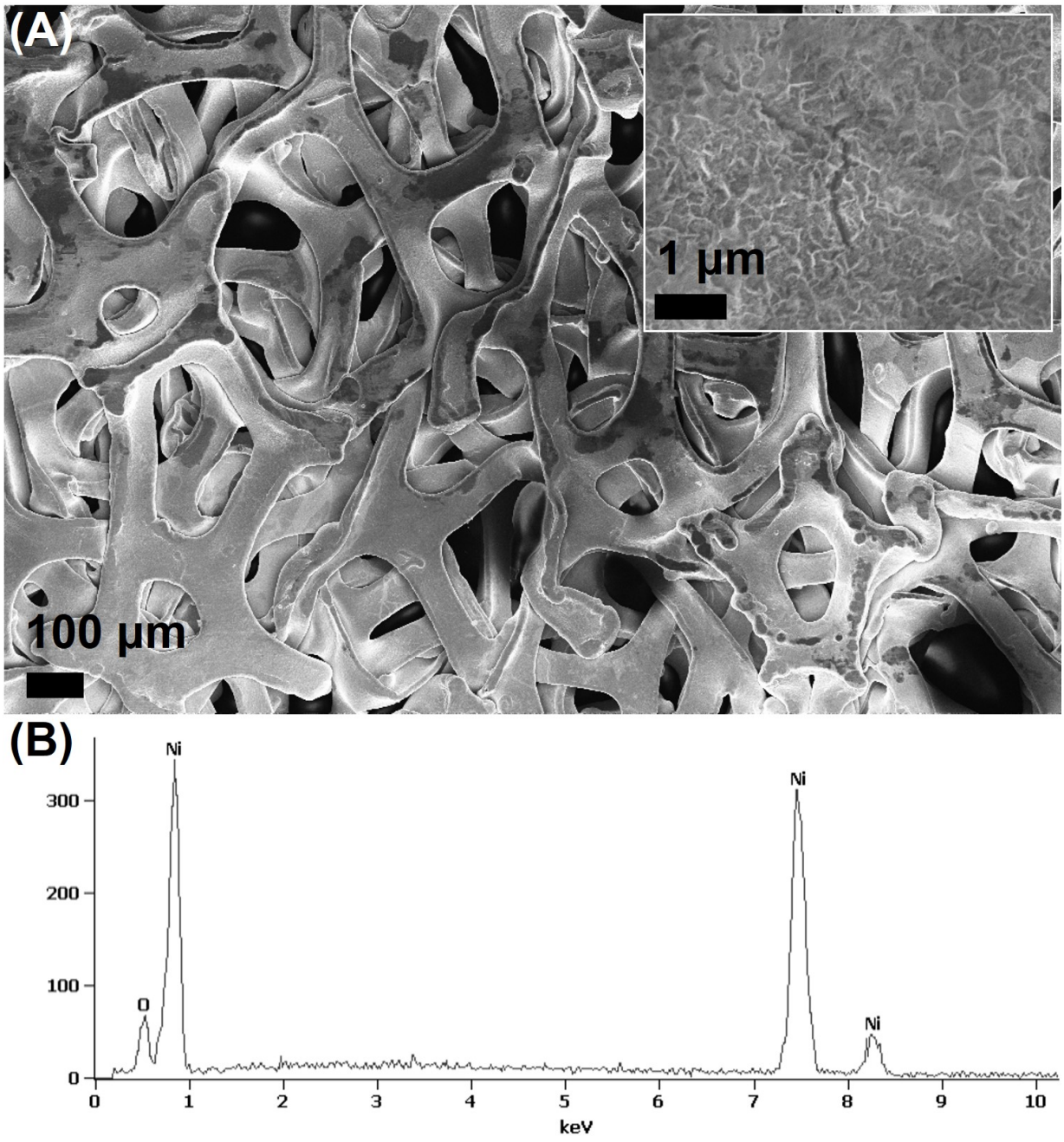

Figure S8: SEM micrograph (A) and EDS spectrum (B) of **Ni_{400}**.

Table S1: Cu:Cl atomic ratios for each **Cu/Ni$_x$** species as obtained from SEM-EDS.

Material	Proposed composition	Atom % Cl (SEM-EDS)	Atom % Cu (SEM-EDS)	Observed Cu:Cl ratio	Expected Cu:Cl ratio
Cu/Ni$_{200}$	$Cu_2(OH)_3Cl$	3.1 ± 0.4	7.0 ± 0.6	2.3(±0.5):1	2:1
Cu/Ni$_{300}$	$Cu_2(OH)_3Cl$	5.5 ± 0.4	13.3 ± 1.2	2.4(±0.4):1	2:1
Cu/Ni$_{400}$	CuO	0.8 ± 0.2	23.8 ± 1.4	29.8(±9.2):1	1:0
Cu/Ni$_{500}$	CuO	0.4 ± 0.0	29.1 ± 0.4	72.8(±1.0):1	1:0
Cu/Ni$_{600}$	CuO	0.4 ± 0.0	26.6 ± 0.4	66.5(±1.0):1	1:0

XPS Analysis and Procedure: For Ni 2p, O 1s and C 1s, ranges for binding energy (BE) values and total number of sweeps were as follows: 848–890 eV, 50–75 sweeps; 525–540 eV, 5–10 sweeps; 278–295 eV, 5–10 sweeps; respectively. The average analysis time for one sample spot was 1.5–2 h. For nickel compounds the spin-orbit splitting of the $2p_{3/2}$ and $2p_{1/2}$ was, in most cases large enough, so that only the more intense $2p_{3/2}$ signal needed be considered. However, overlap of the high BE satellite band from $Ni(OH)_2$ with the $2p_{1/2}$ metal line, which was composed of an asymmetric main line and contributions from plasmon loss structure, could create some challenges in locating appropriate spectral background. The spectrometer dispersion was later adjusted to give a B.E. value of 932.63 eV for metallic Cu $2p_{3/2}$. Charge neutralization was deemed to have been fully achieved by monitoring the C 1s signal for adventitious carbon. A sharp main peak with no lower B.E. structure is generally expected. Instrument base pressure was 7×10^{-9} mbar. High-resolution spectra were obtained using an analysis area of ≈300 × 700 µm and a 20-eV pass energy. This pass energy corresponds to Ag $3d_{5/2}$ full width at half maximum (FWHM) of 0.55 eV (Ref. 48).

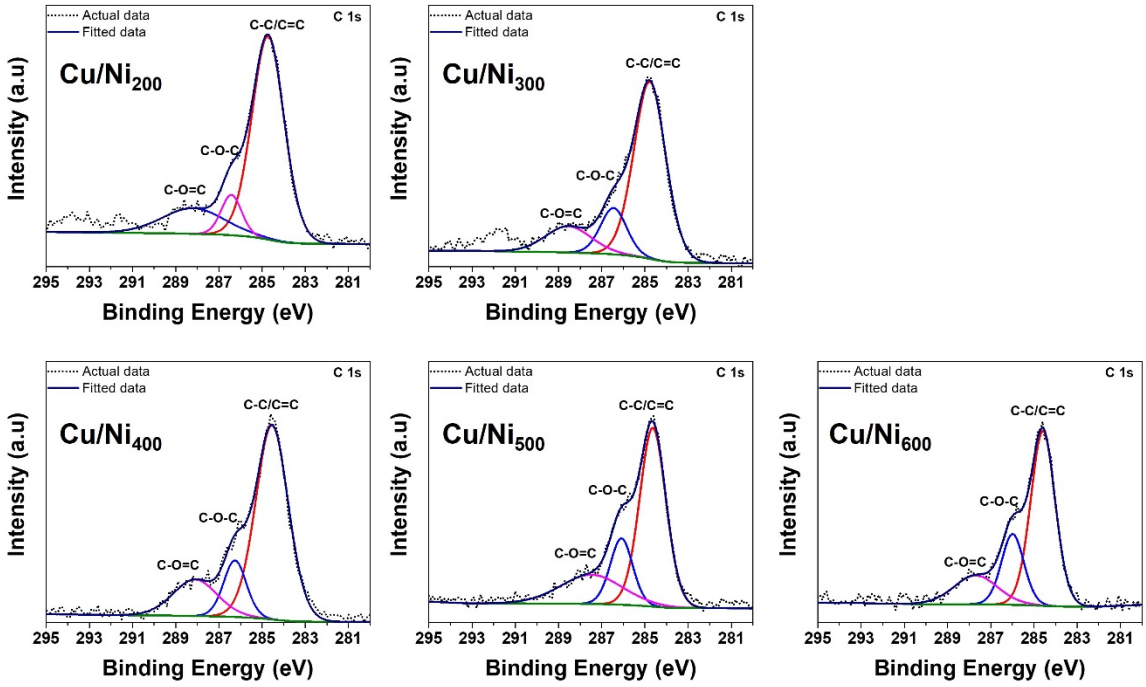

Figure S9: X-ray photoelectron spectra of C 1s for **Cu/Ni$_{200}$** – **Cu/Ni$_{600}$**.

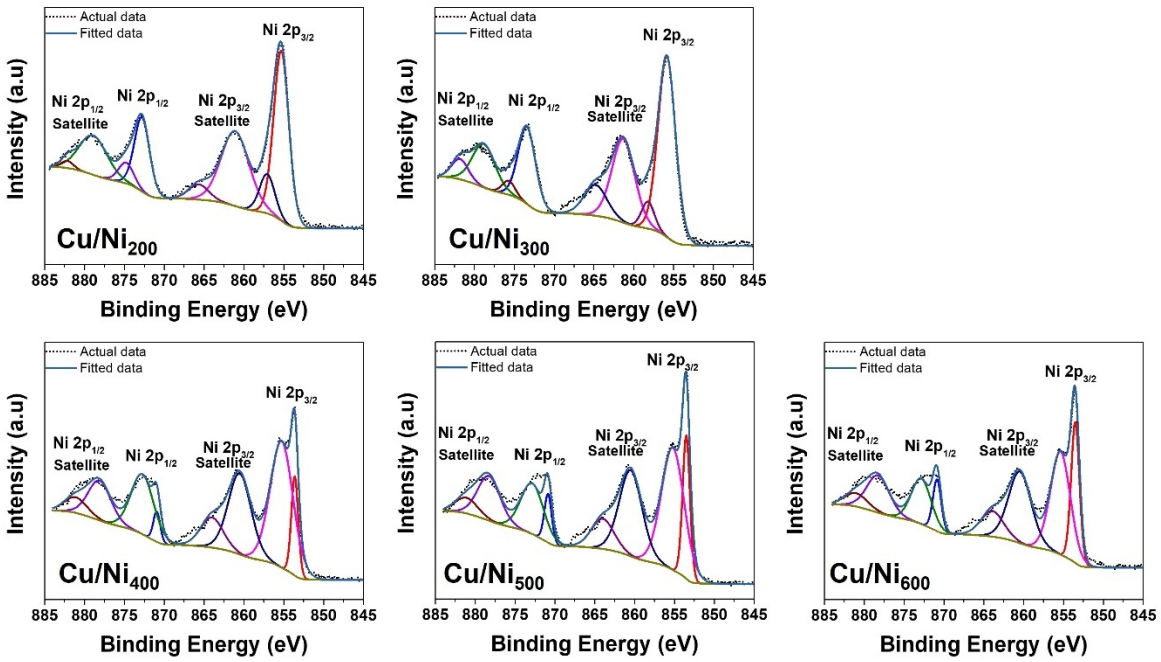

Figure S10: X-ray photoelectron spectra of Ni 2p for **Cu/Ni_{200}** – **Cu/Ni_{600}**.

Table S2: Atomic concentration of elements obtained from survey spectrum.

Sample	C 1s	O 1s	Ni 2p	Cu 2p	Cl 2p
Cu/Ni_{200}	20.22	50.01	17.75	5.49	6.53
Cu/Ni_{300}	21.99	38.65	13.67	9.52	12.99
Cu/Ni_{400}	18.57	48.02	21.81	10.09	1.51
Cu/Ni_{500}	15.39	45.57	24.31	14.73	-
Cu/Ni_{600}	14.97	47.15	21.15	16.74	-
Ni_{400}	20.08	50.6	29.32	-	-

Table S3: Ni 2p binding energy.

Sample	Ni $2p_{3/2}$ peak		Ni $2p_{3/2}$ satellite peak		Ni $2p_{1/2}$ peak		Ni $2p_{1/2}$ satellite peak	
	1st peak B.E.	2nd peak B.E.	1st peak B.E.	2nd peak B.E.	1st peak B.E.	2nd peak B.E.	1st peak B.E.	2nd peak B.E.
Cu/Ni_{200}	855.31	857.01	861.1	865.68	872.8	874.79	878.93	882.16
Cu/Ni_{300}	855.84	864.81	861.3	858.21	873.42	881.82	878.84	875.71
Cu/Ni_{400}	853.62	860.53	855.26	864.02	870.94	878.13	872.73	881.13
Cu/Ni_{500}	853.51	860.49	855.19	864.00	870.87	878.28	872.84	881.11
Cu/Ni_{600}	853.51	860.46	855.37	863.93	870.87	878.27	872.84	881.04
Ni_{400}	854.11	860.84	856.33	864.52	871.91	878.94	872.93	881.74

Table S4: C 1s binding energy values of the prepared catalyst samples.

Sample	C 1s		
	C-C/C=C B.E.	C-O=C B.E.	C-O-C B.E.
Cu/Ni_{200}	284.79	288.30	286.43
Cu/Ni_{300}	284.80	288.59	286.36
Cu/Ni_{400}	284.80	288.21	286.48
Cu/Ni_{500}	284.79	287.56	286.23
Cu/Ni_{600}	284.80	287.89	286.20
Ni_{400}	284.8	288.06	286.79

Table S5: O1s fitted spectra for **Cu/Ni_{200}** – **Cu/Ni_{600}** – see Fig. 4B in manuscript. O 1s binding energy values for the prepared catalyst samples.

Sample	O_L		O_H		O_V		O_C	
	B.E.	**Atomic %**	**B.E.**	**Atomic %**	**B.E.**	**Atomic %**	**B.E.**	**Atomic %**
Cu/Ni_{200}	-	-	531.01	83.04	-	-	532.53	16.96
Cu/Ni_{300}	-	-	531.19	89.52	-	-	532.79	10.48
Cu/Ni_{400}	529.45	48.03	-	-	531.05	42.21	532.56	9.76
Cu/Ni_{500}	529.33	69.45	-	-	531.00	22.40	532.51	8.14
Cu/Ni_{600}	529.40	65.17	-	-	531.10	29.89	532.7	4.94

Table S6: Cu2p fitted spectra for **Cu/Ni$_{200}$** – **Cu/Ni$_{600}$** – see Fig. 4C in manuscript. Cu2p binding energy values for the prepared catalyst samples.

Sample	Cu $2p_{3/2}$ peak				Cu $2p_{3/2}$ satellite peak			
	1st peak	Atomic %	2nd peak	Atomic %	1st peak	Atomic %	2nd peak	Atomic %
	B.E.		B.E.		B.E.		B.E.	
Cu/Ni$_{200}$	934.65	58.40	-	-	943.32	24.00	940.64	17.60
Cu/Ni$_{300}$	934.73	57.97	-	-	943.32	24.54	940.61	17.49
Cu/Ni$_{400}$	934.95	21.15	933.46	40.48	943.51	12.83	940.95	25.54
Cu/Ni$_{500}$	935.11	19.69	933.36	41.11	943.59	11.05	940.99	28.16
Cu/Ni$_{600}$	935.20	18.90	933.47	42.85	943.73	9.76	941.18	28.46

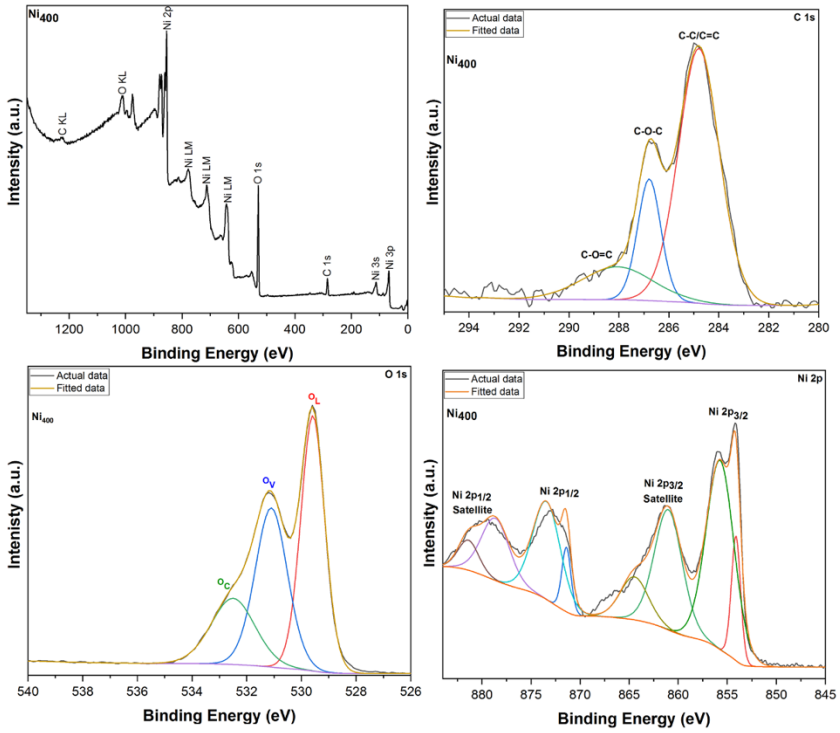

Figure S11: Survey scan (A) and high-resolution spectra of C 1s (B), O 1s (C), and Ni 2p (D) for **Ni$_{400}$**.

The C 1s XPS spectrum for **Ni$_{400}$** indicates the presence of three different species at different BE values. Three different BE values of high-resolution C 1s spectrum obtained by deconvoluting it for three different peaks taking adventitious carbon (C-C/C=C at 284.80 eV) as a reference. The most intense peak observed at 284.80 eV was attributed to the C-C/C=C, while the other peaks visible at 288.06 eV and 286.79 eV were assigned to C-O=C and C-O-C respectively [1]. The deconvoluted O 1s spectrum BE values at 529.58 eV, 531.10 eV, and 532.5 eV were assigned to lattice oxygen (O^{2-}), oxygen vacancy (O_V), and adsorbed oxygen (O_C)respectively. The BE values for O 1s at 529.58 eV suggested the presence of metal oxygen bonds [2].

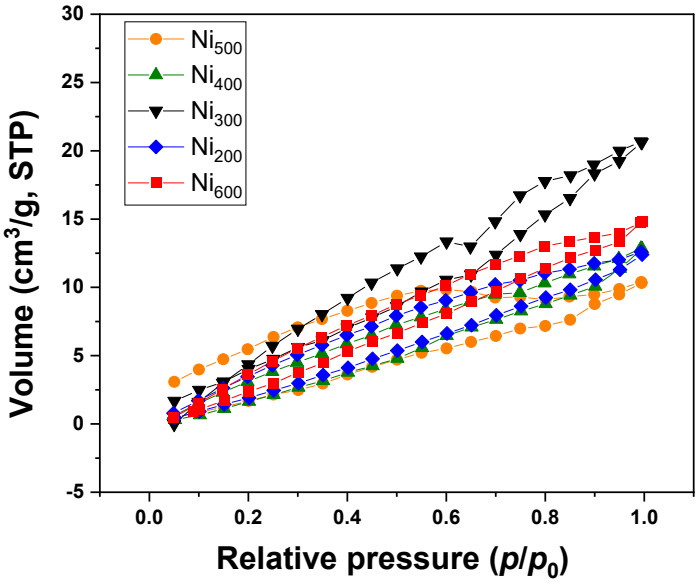

Figure S12: N_2 adsorption-desorption isotherms for the bare **Ni_x** samples.

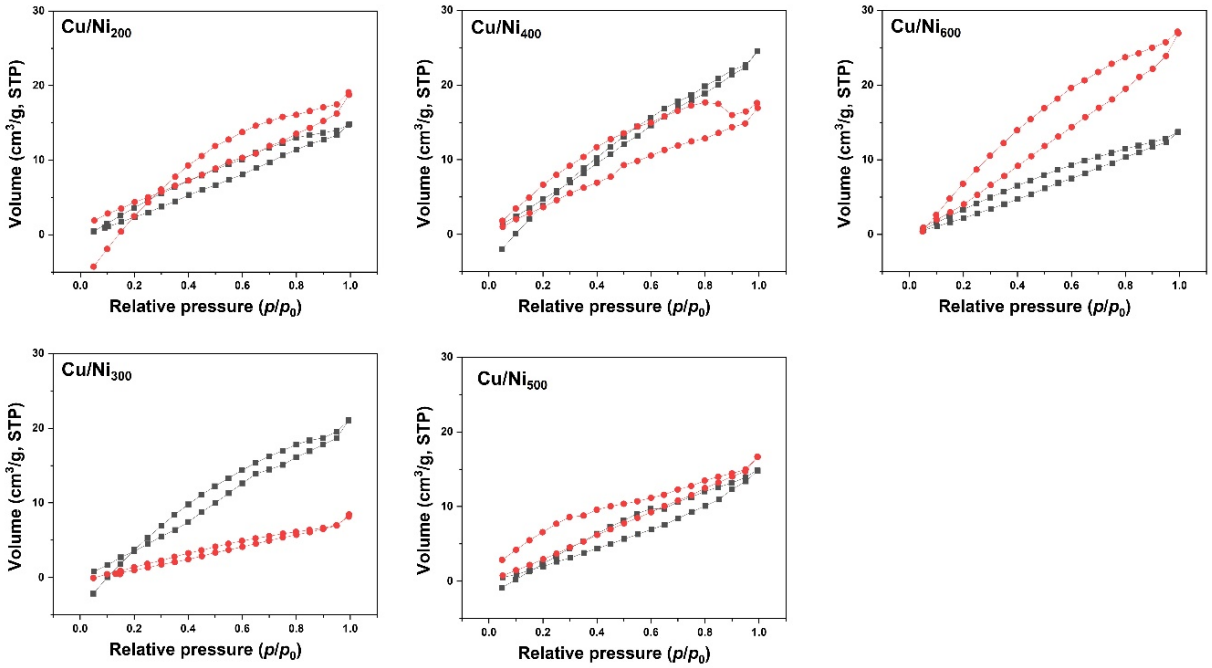

Figure S13: N_2 adsorption-desorption isotherms for each **Cu/Ni$_x$** sample.

Table S8: Cu/Ni$_x$ surface areas obtained from BET method.

Material	Surface area of Ni$_x$ (m^2g^{-1})	(i) Surface area of Cu/Ni$_x$ (m^2g^{-1})	(ii) Surface area of Cu/Ni$_x$ (m^2g^{-1})	Avg. Surface area of Cu@/Ni$_x$ (m^2g^{-1})	Δ Surface Area [Avg. Cu/Ni$_x$ - Ni$_x$](m^2g^{-1})	Normalized Surface area for Cu catalyst component (*See Table 1 - manuscript*) (m^2g^{-1})
Cu/Ni$_{200}$	19.62	29.76	19.66	24.71	5.09	202.41 ± 119.21
Cu/Ni$_{300}$	21.70	24.38	35.93	30.15	8.45	184.42 ± 126.05
Cu/Ni$_{400}$	16.52	34.70	28.58	31.64	15.12	842.09 ± 170.27
Cu/Ni$_{500}$	14.28	20.01	27.01	23.51	9.22	689.35 ± 261.70
Cu/Ni$_{600}$	19.36	21.22	46.72	33.97	14.61	885.90 ± 319.32

Catalysis Trials

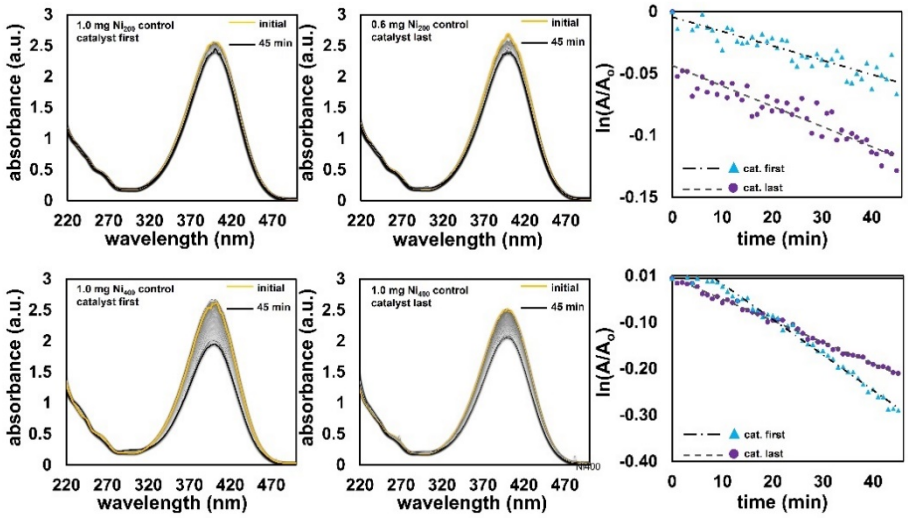

Figure S14: Catalytic reduction of **4NP** (0.39 µmol) in 3 mL DIW with 0.2 mmol $NaBH_4$ with **Ni$_{200}$** [1] and **Ni$_{400}$** (*bottom*) with addition order of catalyst first. Change of absorbance was monitored at 1 min intervals.

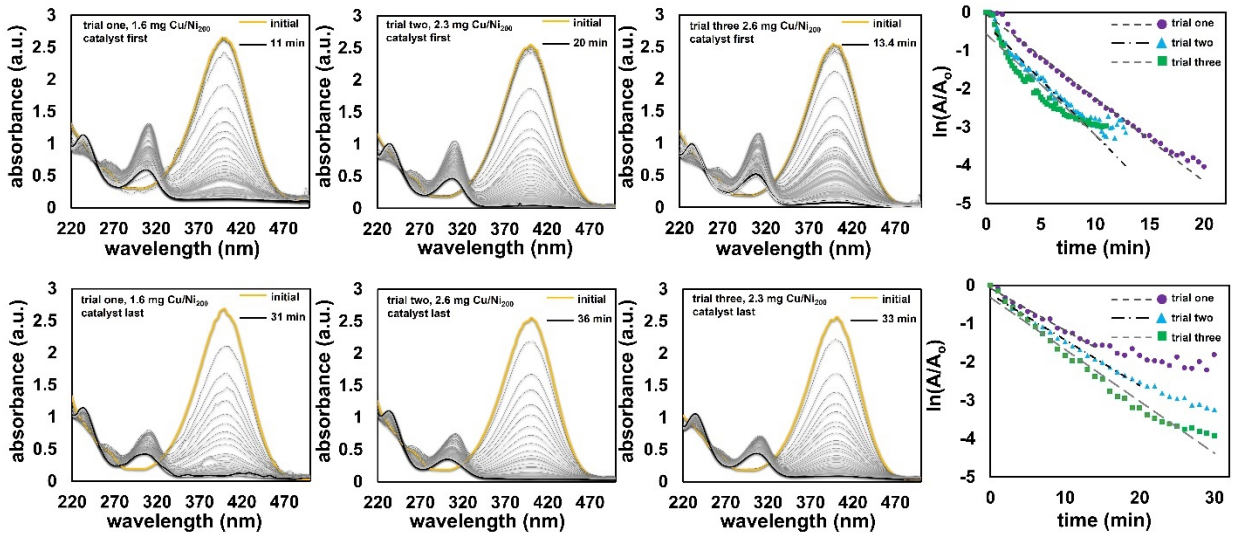

Figure S15: Catalytic reduction of **4NP** (0.39 µmol) in 3 mL DIW with 0.2 mmol $NaBH_4$ with **Cu/Ni_{200}** with catalyst order of addition first and last (*bottom*). Change of absorbance was monitored at 0.5, 0.2, and 0.2 min intervals for catalyst first (left to right) and 1 min intervals for catalyst last trials. Perturbation from evolved H_2 bubbles was normalized to a flat baseline.

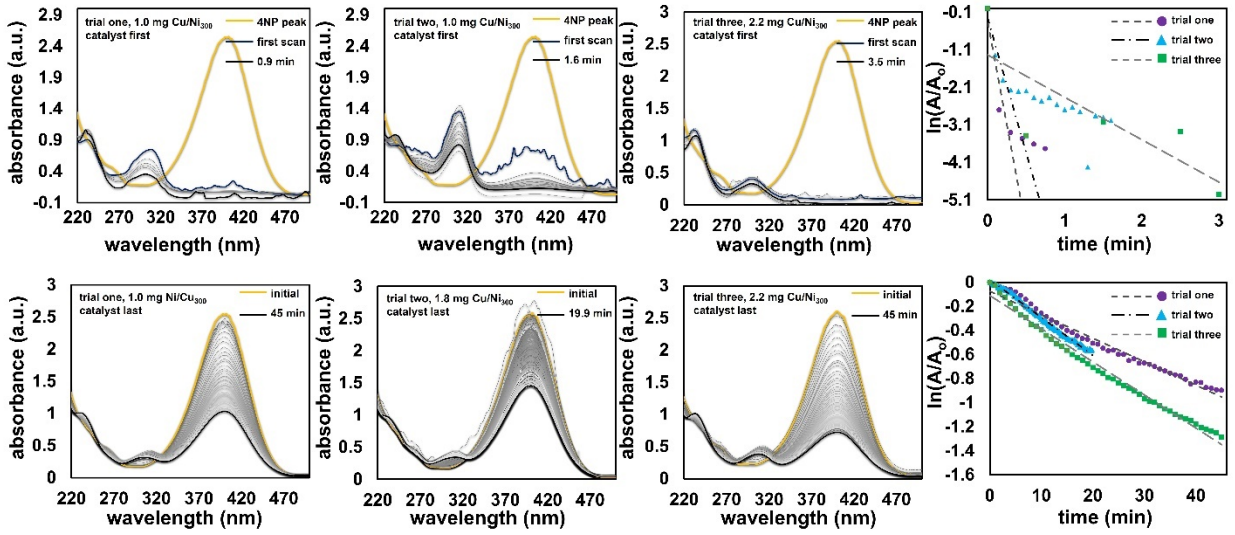

Figure S16: Catalytic reduction of **4NP** (0.39 µmol) in 3 mL DIW with 0.2 mmol $NaBH_4$ with **Cu/Ni_{300}** with catalyst order of addition first and last (*bottom*). Change of absorbance was monitored at 0.1, 0.1, and 0.5 min intervals for catalyst first (left to right) and 1, 0.1, and 1 min intervals for catalyst last trials (left to right). Perturbation from evolved H_2 bubbles was normalized to a flat baseline.

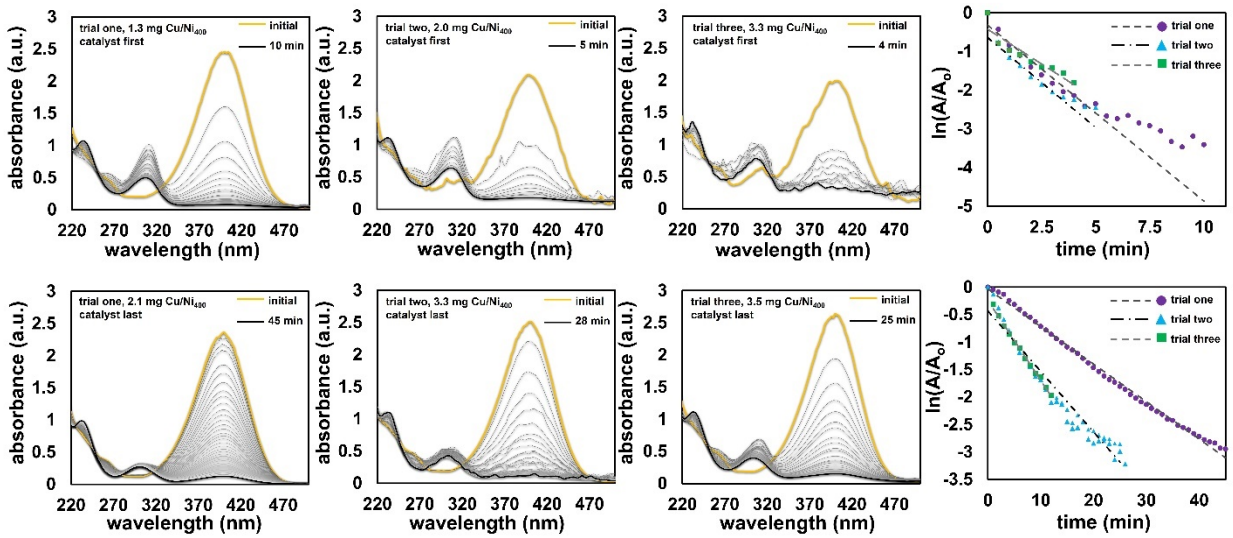

Figure S17: Catalytic reduction of **4NP** (0.39 µmol) in 3 mL DIW with 0.2 mmol $NaBH_4$ with **Cu/Ni$_{400}$** with catalyst order of addition first and last (*bottom*). Change of absorbance was monitored 0.5 min intervals for catalyst first and 1 min intervals for catalyst last trials. Perturbation from evolved H_2 bubbles was normalized to a flat baseline.

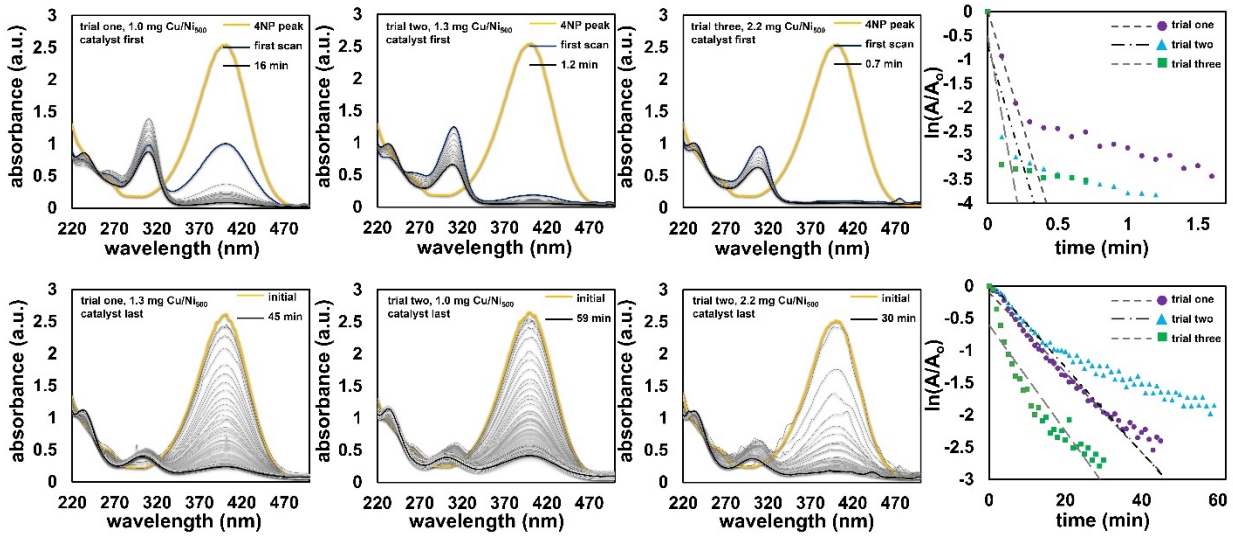

Figure S18: Catalytic reduction of **4NP** (0.39 µmol) in 3 mL DIW with 0.2 mmol $NaBH_4$ with **Cu/Ni$_{500}$** with catalyst order of addition first and last (*bottom*). Change of absorbance was monitored at 0.1 min intervals for catalyst first and 1 min intervals for catalyst last trials. Perturbation from evolved H_2 bubbles was normalized to a flat baseline.

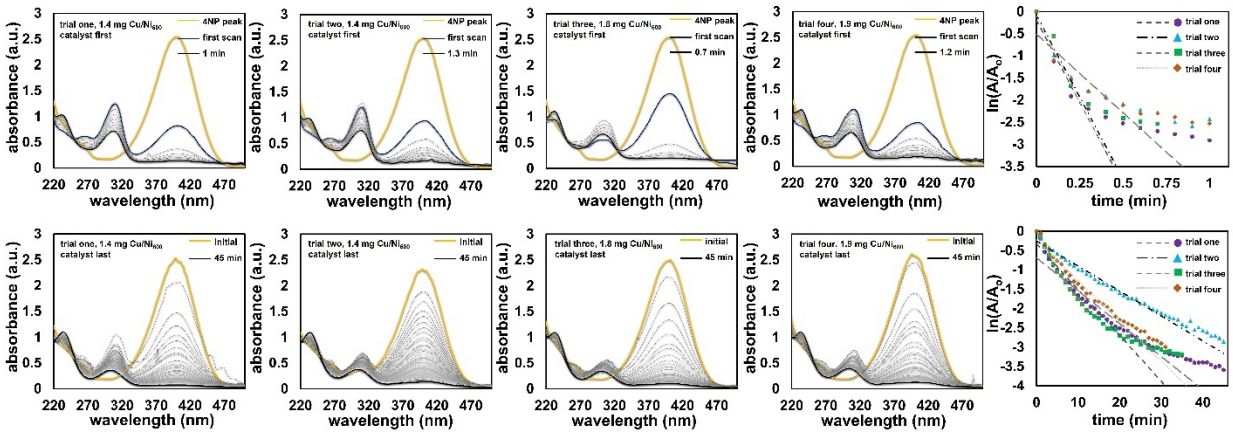

Figure S19: Catalytic reduction of **4NP** (0.39 µmol) in 3 mL DIW with 0.2 mmol $NaBH_4$ with **Cu/Ni$_{600}$** with catalyst order of addition first and last (*bottom*). Change of absorbance was monitored at 0.1 min intervals for catalyst first and 1 min intervals for catalyst last trials. Perturbation from evolved H_2 bubbles was normalized to a flat baseline.

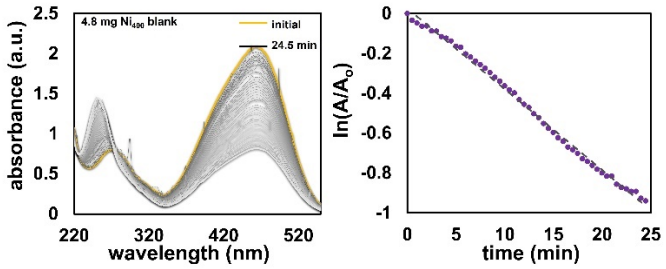

Figure S20: Catalytic reduction of **MO** (0.34 µmol) in 3 mL DIW with 0.2 mmol $NaBH_4$ with **Ni$_{400}$**. Change of absorbance was monitored at 0.5 min intervals.

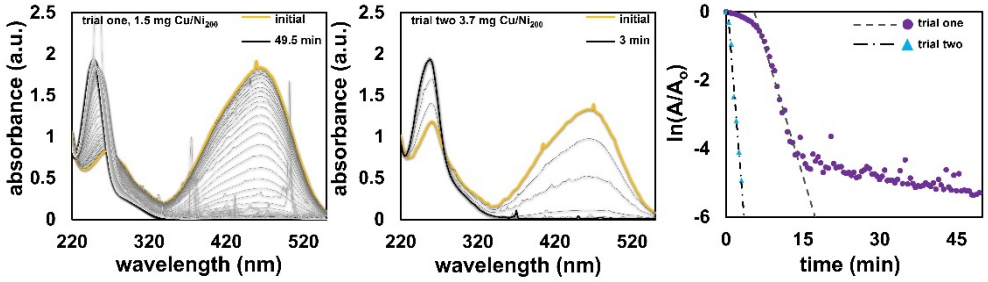

Figure S21: Catalytic reduction **MO** (0.34 µmol) in 3 mL DIW with 0.2 mmol $NaBH_4$ with **Cu/Ni$_{200}$** with catalyst added last. Change of absorbance was monitored at 0.5 min intervals.

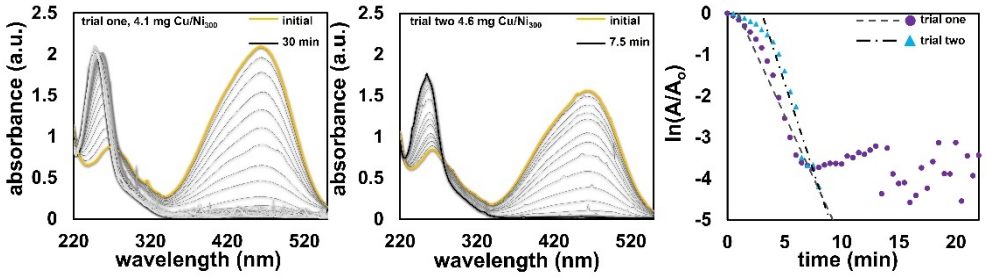

Figure S22: Catalytic reduction **MO** (0.34 µmol) in 3 mL DIW with 0.2 mmol $NaBH_4$ with **Cu/Ni$_{300}$** with catalyst added last. Change of absorbance was monitored at 0.5 min intervals.

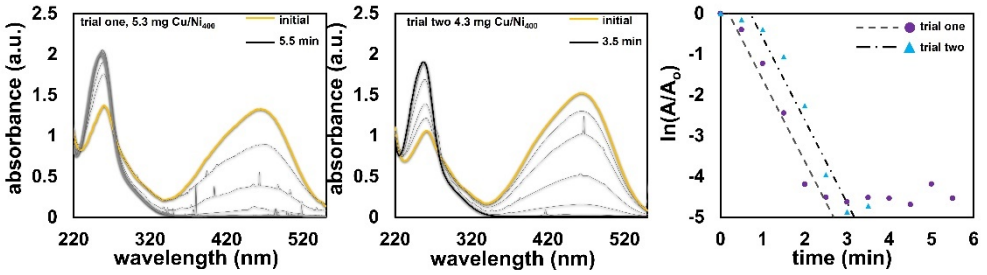

Figure S23: Catalytic reduction **MO** (0.34 µmol) in 3 mL DIW with 0.2 mmol $NaBH_4$ with **Cu/Ni$_{400}$** with catalyst added last. Change of absorbance was monitored at 0.5 min intervals.

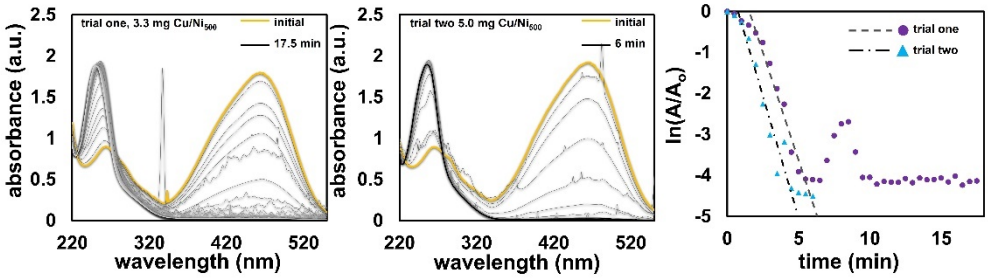

Figure S24: Catalytic reduction **MO** (0.34 µmol) in 3 mL DIW with 0.2 mmol $NaBH_4$ with **Cu/Ni$_{500}$** with catalyst added last. Change of absorbance was monitored at 0.5 min intervals.

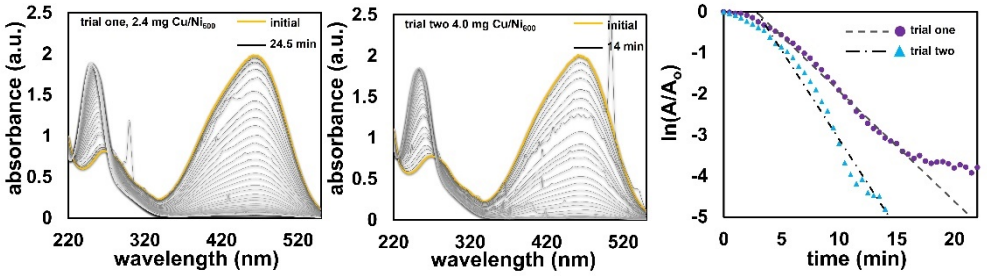

Figure S25: Catalytic reduction **MO** (0.34 µmol) in 3 mL DIW with 0.2 mmol $NaBH_4$ with **Cu/Ni$_{600}$** with catalyst added last. Change of absorbance was monitored at 0.5 min intervals.

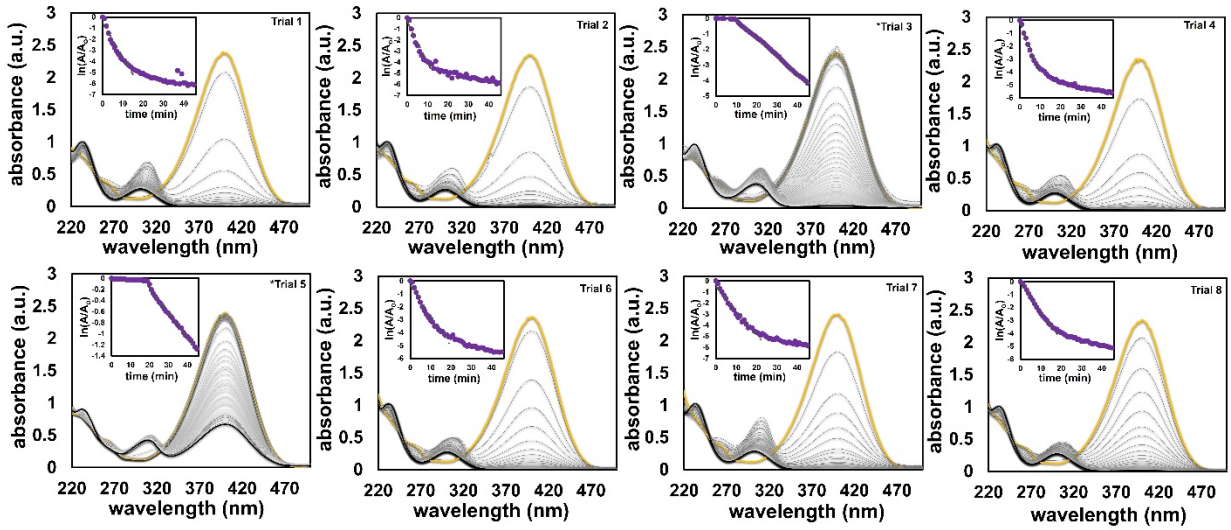

Figure S26: Catalytic recycling trials for the reduction of **4NP** (0.39 µmol) in 3 mL DIW with 0.2 mmol $NaBH_4$ with **Cu/Ni$_{500}$** with catalyst added last. of **4NP→4AP*** in DIW with excess $NaBH_4$. Recycling trials 1,2,4,6-8 were rinsed thoroughly with DIW, trials 3 and 5, were only cleaned with one quick DIW rinse which resulted in reduced rate and a notable induction period. Change of absorbance was monitored at 0.1 min intervals.

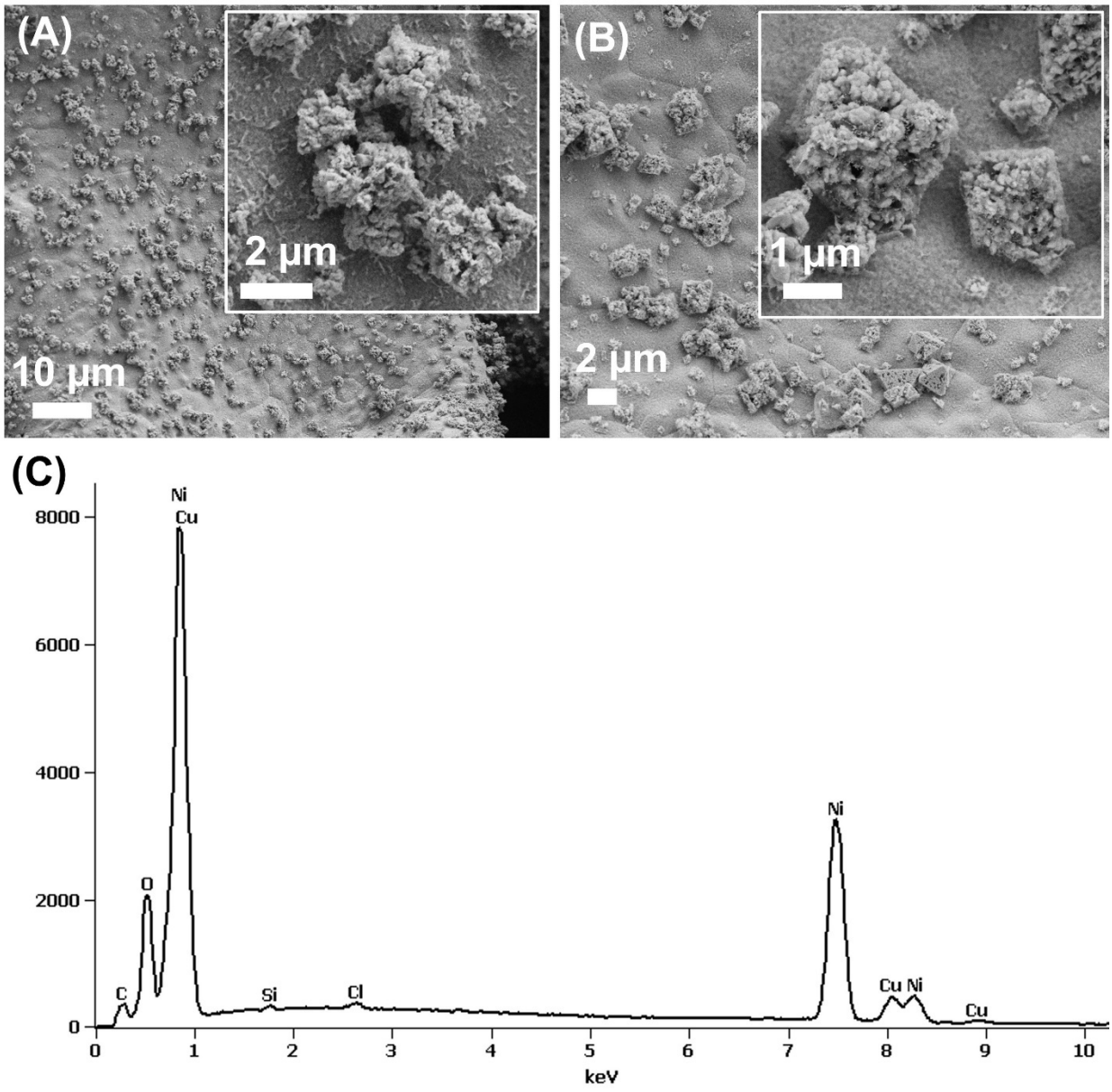

Figure S27: SEM micrograph of post-mortem **Cu/Ni$_{400}$** (A) and **Cu/Ni$_{500}$** (B), and EDS spectrum (C) of **Cu/Ni$_{400}$** post-mortem.

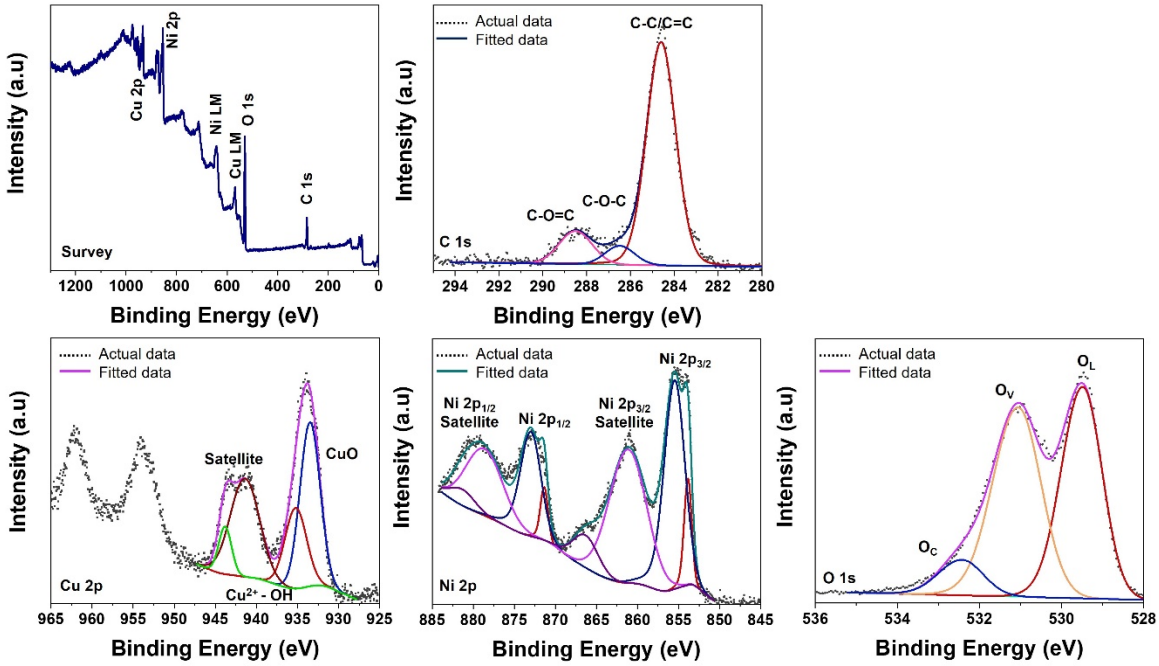

Figure S28: X-ray photoelectron spectra for **Cu/Ni$_{400}$** post-mortem.

Table S9: Atomic concentration of elements obtained from survey spectrum for **Cu/Ni$_{400}$** post-mortem sample.

Sample	C 1s	O 1s	Ni 2p	Cu 2p	Cl 2p	N 1s	B 1s	Na 1s
Spent Cu/Ni$_{400}$ At.%	31.79	40.45	15.39	8.21	1.79	0.58	1.79	0

References:

1. Landoulsi, J., et al.Organic adlayer on inorganic materials: XPS analysis selectivity to cope with adventitious contamination. *Applied Surface Science* **2016**, 383, 71-83.
2. Biesinger, M.C.Advanced analysis of copper X-ray photoelectron spectra. *Surface and Interface Analysis* **2017**, 49, 1325-1334.